

Enhanced diffusion of molecular hydrogen in germanosilicate fibres loaded with hydrogen at high pressures

S.A. Vasil'ev, A.O. Rybaltovskii, V.V. Koltashev, V.O. Sokolov, S.N. Klyamkin, O.I. Medvedkov, A.A. Rybaltovskii, A.R. Malosiev, V.G. Plotnichenko, E.M. Dianov

Abstract. Absorption spectra and spontaneous Raman spectra of optical fibres with a germanosilicate core loaded with molecular hydrogen at a pressure of 150–170 MPa are studied; the variation of these spectra during the outdiffusion of hydrogen from the fibres is also investigated. The purely rotational transitions of molecular hydrogen in Raman spectra of optical fibres are recorded for the first time. The changes in the spectral parameters of fibre Bragg gratings loaded with hydrogen are analysed. It is observed for the first time that under such high loading pressures, the decrease in the hydrogen concentration in the fibre core after completion of hydrogen loading occurs in two clearly manifested stages, the initial stage being characterised by a more rapid outlet of hydrogen as compared to the dynamics of hydrogen outdiffusing at pressures of 10–15 MPa. Barodiffusion of molecular hydrogen in optical fibres is considered as the main mechanism explaining this effect. An increase in the solubility of molecular hydrogen in germanosilicate fibres exposed to UV radiation is observed for the first time.

Keywords: optical fibre, diffusion, barodiffusion, molecular hydrogen, refractive index grating.

1. Introduction

The keen interest towards the investigation of spectral parameters of molecular hydrogen and its interaction with high-purity silica ($v\text{-SiO}_2$) and germanosilicate (GS) $\text{GeO}_2\text{-SiO}_2$ glass networks during the past twenty years stems mainly from the following circumstances. First, the loading of fibres with H_2 molecules into such fibres leads to elevated optical losses in the telecommunication wavelength range (1.0–1.7 μm) due to the appearance of vibrational

absorption bands of H_2 molecules and hydroxyl (OH) groups [1, 2]. Second, this interest is stimulated by the research in the field of photoinduced processes occurring in glass networks involving molecular hydrogen; the presence of hydrogen increases the photosensitivity of optical fibres in many cases during the refractive index grating recording in them [3, 4] (photosensitivity depends on the concentration of hydrogen dissolved in the glass). A record-high induced refractive index ($\Delta n > 0.01$) [5] was reported in single-mode GS fibres loaded with hydrogen under a pressure of 200 MPa and exposed to UV radiation from a KrF laser. It is assumed that the a considerable increase in the writing efficiency of refractive index gratings by UV radiation in hydrogen-loaded GS fibres is due to the formation of OH and Ge–H groups as well as GeE' centres in photochemical reactions with H_2 molecules [6, 7]. Regions with an increased concentration of Ge–Ge bonds and germanium nanocrystals, which are formed in the glass network, can make a certain contribution to this process [8].

To determine the limiting solubility of hydrogen in the silica network and the concentration dependence of the thermochemical and photochemical reactions involving H_2 molecules, it is expedient to study the properties of molecular hydrogen dissolved in the glass network under loading pressures exceeding 100 MPa. So far, only a few authors [5, 9, 10] have discussed various aspects of the spectral manifestation of the physical properties of H_2 molecules in the pure silica network and GS glasses loaded with hydrogen at such high pressures.

In this paper, we study by the methods of absorption and Raman spectroscopy the spectral properties of molecular hydrogen dissolved in the germanosilicate glass network at pressures of 150–170 MPa. Such studies were initiated by the authors of [8, 10, 11] at lower loading pressures.

To obtain information about the state of molecular hydrogen, its concentration and interaction with the glass network, we studied the spectral position, intensity and the width of Raman lines and the 1.24- μm absorption band of hydrogen, during its outlet from the optical fibre. The change in the H_2 concentration in the fibre core was also controlled from the shift of the reflection peak of fibre Bragg gratings (FBGs) [12], written preliminarily in the fibres under investigation.

2. Investigated samples and measuring techniques

We studied single-mode optical fibres with a GS glass core with various concentrations of germanium. By using such samples with a large length and a small cross section, we

S.A. Vasil'ev, V.V. Koltashev, V.O. Sokolov, O.I. Medvedkov, A.A. Rybaltovskii, V.G. Plotnichenko, E.M. Dianov Fibre Optics Research Center, A.M. Prokhorov General Physics Institute, Russian Academy of Sciences, ul. Vavilova 38, 119991 Moscow, Russia; e-mail: sav@fo.gpi.ru;

A.O. Rybaltovskii D.V. Skobel'tsyn Institute of Nuclear Physics, M.V. Lomonosov Moscow State University, Vorob'evy gory, 119992 Moscow, Russia;

S.N. Klyamkin Department of Chemistry, M.V. Lomonosov Moscow State University, Vorob'evy gory, 119992 Moscow, Russia;

A.R. Malosiev Department of Physics, M.V. Lomonosov Moscow State University, Vorob'evy gory, 119992 Moscow, Russia

Received 27 September 2004

Kvantovaya Elektronika 35 (3) 278–284 (2005)

Translated by Ram Wadhwa

were able to load glasses with hydrogen to high concentrations (up to $3 \times 10^{21} \text{ cm}^{-3}$) at temperatures below 100°C and to observe purely rotational (the S_0 branch) Raman transitions in H_2 molecules with a small scattering cross section.

We investigated single-mode optical fibres with a GS glass core, whose parameters are presented in Table 1. All the fibres, except Corning Flexcor-1060, were prepared by the MCVD technique at the Institute of High-Purity Substances, Russian Academy of Sciences, Nizhnii Novgorod and at the Fibre Optics Research Center, A.M. Prokhorov General Physics Institute, Russian Academy of Sciences, Moscow.

Table 1. Parameters of investigated fibres.

Fibre No.	Brand	Core diameter/ μm	Molar concentration of GeO_2 in the core (%)	Loading pressure/MPa
1	88ch	2.7	19	150
2	Corning Flexcor-1060	4.7	4.5	150
3	Ge113	3.2	14	150
4	SM727cf	3.4	13	150
5	SM921	2.5	24	170

The diameter of cladding of all fibres was $125 \mu\text{m}$. Fibres were hydrogen-loaded in a special chamber under a pressure of $150\text{--}170 \text{ MPa}$ for 24 hours at a temperature of 100°C . Estimates using the diffusion coefficient borrowed from [1] show that the hydrogen concentration in the core as a result of such a treatment should be at least 99.95 % of its value in the peripheral regions of the fibre.

Before loading with hydrogen, FBGs were written in some fibres. In fibre sample Nos 2 and 3, FBGs were written by using a CL-5000 excimer ArF laser ($\lambda = 193 \text{ nm}$) through a phase mask [13], while for sample Nos 4 and 5 the second harmonic of an Ar⁺ laser ($\lambda = 244 \text{ nm}$) was used in a scheme with a Lloyd interferometer [14]. The fibres were not hydrogen-loaded before FBG writing. The FBG length was 5 mm and the resonance wavelength was in the region of the emission maximum ($\sim 1330 \text{ nm}$) of the luminescence diode used in experiments. The two types of gratings were written: type I (in fibres with a molar concentration of GeO_2 lower than 15%) and type IIa (in fibres with a molar concentration of GeO_2 higher than 15%) [15]. Before loading with hydrogen, polymer coating was restored in regions where FBGs were written.

The time interval between opening of the hydrogen chamber and the beginning of measurements varied between 1.5 and 5 hours. Unless specially stated otherwise, all spectral measurements were made at room temperature. Typical length of the fibre samples being tested was 1 m.

Raman spectra were excited in the fibres by the 514.5-nm line of an Ar laser through a microscope and were measured in the frequency range $10\text{--}5000 \text{ cm}^{-1}$ with a T-64000 Jobin Yvon spectrograph equipped with a CCD camera. The spectra were normalised to the intensity of the main Raman band of GS glasses at $\sim 430 \text{ cm}^{-1}$.

Parameters of the $1.24\text{-}\mu\text{m}$ absorption band were measured with a spectrum analyser simultaneously with the recording of the spectral properties of FBGs. The absorption band and FBG spectra were recorded with a resolution of 2 and 0.1 nm, respectively.

3. Results of measurements and discussion

3.1 Raman spectra

Figure 1 shows the Raman spectra for fibre No. 1 before loading with hydrogen under a pressure of 150 MPa and 5 hours after hydrogen loading (for comparison, the spectra were normalised to the maximum of the Q_1 band). One can see that the Raman spectrum of the hydrogen-loaded fibre exhibits an almost symmetric intense band at 4141 cm^{-1} and a number of weaker bands in the frequency interval $300\text{--}1100 \text{ cm}^{-1}$ superimposed on Raman bands belonging to the GS glass. According to the results obtained in [10, 11], the Raman band at 4141 cm^{-1} belongs to the Q_1 branch ($\Delta v = 1, \Delta J = 0$), while the bands at $337, 590, 817$ and 1030 cm^{-1} belong to the purely rotational transitions of the S_0 branch ($\Delta v = 0, \Delta J = 2$) of H_2 molecules in the glass network.

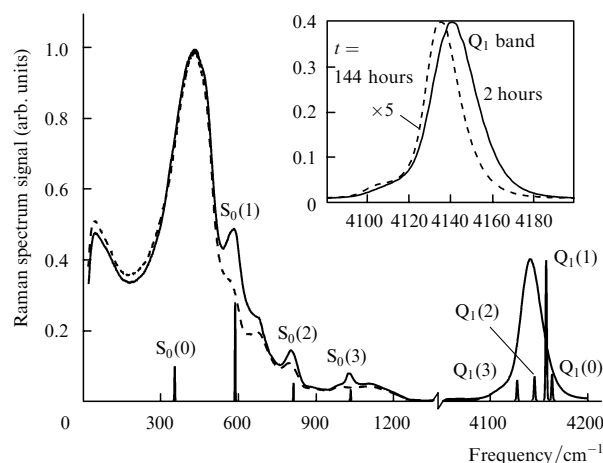


Figure 1. Raman spectra of optical fibre No. 1 before (dashed curve) and 5 hours after (solid curve) loading with hydrogen at a pressure of 150 MPa . The line spectrum is the Raman spectrum of molecular hydrogen in gaseous state at a pressure of 0.2 MPa . The inset shows the Q_1 band of H_2 molecules measured 2 hours (solid curves) and 144 hours (dashed curve) after hydrogen loading. For convenience of comparison, the intensity of the spectrum measured after 144 hours is magnified five times.

For comparison, Fig. 1 shows the Raman spectrum of molecular hydrogen in gaseous state under a pressure of about 0.2 MPa . Table 2 shows the frequencies of the Raman bands and their classification for gaseous hydrogen (for $P = 0.2 \text{ MPa}$ and $T = 300 \text{ K}$) and hydrogen dissolved in the silica glass network.

Note that hydrogen loading at high pressures allowed us to observe clearly for the first time the lines of purely rotational S_0 transitions of molecular hydrogen dissolved physically in the silica glass network. In contrast to the pronounced lines $S_0(1)$, $S_0(2)$ and $S_0(3)$, the rotational $S_0(0)$ transition in the Raman spectrum in a GS fibre (Fig. 1) is manifested as an inflection on the low-frequency wing of the main Raman band of the glass network. As in the case of Raman spectrum of gaseous hydrogen, the component $S_0(1)$ belonging to ortho- H_2 has the highest intensity among all the observed purely rotational bands in the Raman spectra of optical fibres. However, even the intensity of this band is not sufficient for quantitative intensity measurements. This

Table 2. Frequencies of Raman bands of molecular hydrogen/cm⁻¹.

Branch	S ₀ (0)	S ₀ (1)	S ₀ (2)	S ₀ (3)	Q ₁ (0)	Q ₁ (1)	Q ₁ (2)	Q ₁ (3)
H ₂ dissolved in the glass network [8, current publication]	337	590	817	1030	Single band at 4141 cm ⁻¹			
Gaseous H ₂ [10]	354.381	587.055	814.406	1034.651	4161.134	4155.201	4143.387	4125.832

circumstance and the partial overlap of the purely rotational bands with the Raman bands related to the glass network vibrations (for example, at 606 and 800 cm⁻¹) prevented a detailed study of the dynamics of their variation with the outlet of hydrogen from the fibre.

We observed the 4141-cm⁻¹ Q₁ band earlier [8] at a frequency of 4136 cm⁻¹ in GS fibres loaded with hydrogen under a pressure of 10–12 MPa. This band and its variation with the outlet of hydrogen from the fibre are shown in the inset to Fig. 1. It can be seen that as the concentration of hydrogen decreases, the Q₁ band shifts to the red while its shape changes from nearly symmetric to asymmetric with a pronounced low-frequency component. The presence of the asymmetric Raman band was reported earlier in [10, 11] where the Raman spectra of hydrogen-loaded pure silica glasses were studied.

3.2 The 1.24-μm absorption band

An increase in the concentration of hydrogen in GS fibres loaded with hydrogen at pressures 150–170 MPa compared to its concentration at pressures 10–20 MPa leads to a change in the parameters of the 1.24-μm absorption band related to the first overtone of vibrational Q₁ band of molecular hydrogen [2], which is used, as a rule, for determining the concentration of hydrogen in optical fibres (Fig. 2). The intensity of this band after hydrogen loading at pressures 150–170 MPa depends on the properties of the fibre, and was found to be equal to 8–9 dB m⁻¹ in the samples investigated by us.

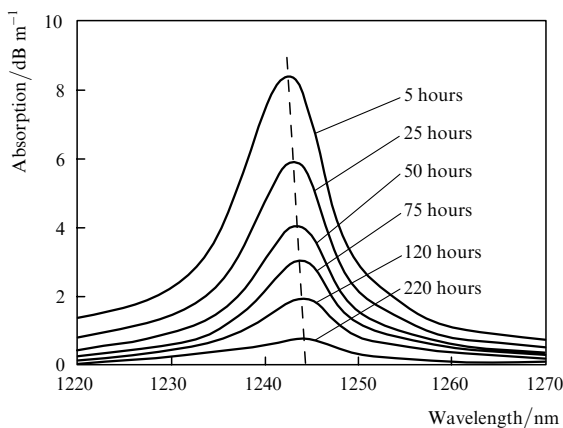


Figure 2. Absorption spectra of molecular hydrogen at 1.24 μm, measured in fibre No. 4 after the indicated time intervals following hydrogen processing at a pressure of 170 MPa.

Assuming that the concentration of hydrogen is proportional to the intensity of the 1.24-μm absorption band and using the results obtained in [1] for hydrogen-loading pressures of ~0.1 MPa, we estimated the molar concentration of H₂ molecules in our samples at about 10%–11%, or ~3 × 10²¹ cm⁻³. Note that the intensity of the 1.24-μm band remains nearly proportional to the hydrogen

pressure in the chamber even for high loading pressures. At the same time, a tendency towards absorption saturation is observed. Departure from the linear dependence at a pressure of 170 MPa is 20%–30%, which exceeds the error of our measurements (5%). This is in good agreement with the results obtained in [5, 10], where such measurements were performed at pressures up to 150–200 MPa. Departure from the linear dependence may be due to the fact that an increase in the hydrogen pressure in the chamber enhances the interaction of dissolved H₂ molecules with the glass network and with one another. In our opinion, the latter circumstance must be taken into account in spite of the fact that the average number of H₂ molecules in the interstices of the network is still below unity for concentrations ~3 × 10²¹ cm⁻³.

Note that a decrease in the concentration of hydrogen dissolved in the glass is accompanied by a slight shift of the absorption band from 1.242 μm (5 hours after loading with hydrogen) to 1.244 μm (after 220 hours). This can be seen clearly in Fig. 2 (dashed line). The relative shift of this band (~0.1%) approximately corresponds to the measured relative shift of the Q₁ band in the Raman spectrum (see inset in Fig. 1).

For high loading pressures, we observed a change in the dynamics of the outlet of molecular hydrogen from the fibre. According to the diffusion equation describing the outlet of hydrogen from the fibre and assuming that the diffusion coefficient is independent of pressure, the relative variation in hydrogen concentration along the fibre axis must be independent of loading pressure (initial hydrogen concentration). This means that the dependences of the hydrogen outlet measured at various loading pressures must be identical. This condition is satisfied quite well for low loading pressures. However, it was found that the dependences of the hydrogen outlet measured at high loading pressures are no longer identical.

This fact is illustrated in Fig. 3 showing the time dependence of the amplitude of the 1.24-μm absorption band after hydrogen loading. These dependences were measured for fibre No. 4 at pressures of 150 and 12.5 MPa in the chamber. The dependence measured at low pressure is multiplied by 5.3 (the absorption peak amplitude during the first hours of the measurement was about 0.8 dB m⁻¹) for a better matching of the two dependences at time periods exceeding 50 hours. One can see from Fig. 3 that the absorption decay curves differ significantly from one another at the initial period of time (below 50 hours): the absorption, and hence the relative concentration, of hydrogen along the fibre axis decreases much more rapidly at high loading pressures than at low pressures.

In addition, the dashed curve in Fig. 3 shows the time dependence of the hydrogen concentration along the fibre axis calculated by solving the time-dependent diffusion equation with a constant diffusion coefficient $D_{H_2} = 2.5 \times 10^{-11}$ cm² s⁻¹ at a temperature of 25 °C [1]. One can see that such a calculation is in good agreement with the measurements made at low loading pressures

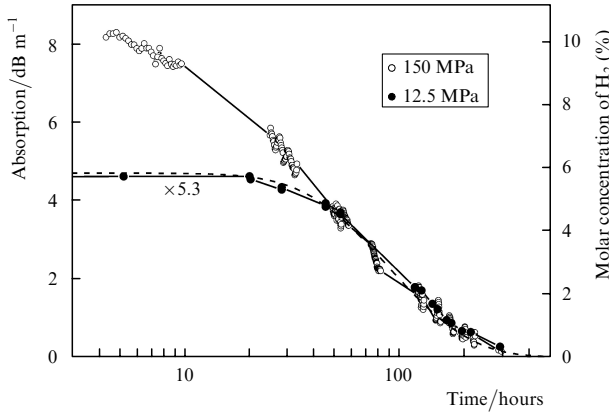


Figure 3. Amplitude of the 1.24- μm absorption band as a function of time of hydrogen outlet from fibre No. 4 at a loading pressure of 150 and 12.5 MPa. The dashed curve is the calculation of the hydrogen outlet for a constant diffusion coefficient.

(both dependences contain an initial segment with a nearly constant concentration of hydrogen). The latter circumstance is due to the fact that molecular hydrogen leaves the cladding region during the initial time interval, and hydrogen concentration starts decreasing in the fibre core only after a certain interval of time depending on the diameter of the fibre cladding and temperature. For a cladding diameter of 125 μm , a noticeable decrease in hydrogen concentration along the fibre axis at room temperature occurs about 20–30 hours after hydrogen loading. However, it can be seen from Fig. 3 that for high loading pressures, the length of the initial segment drops to 3–5 hours, thus pointing towards an increase in the diffusion coefficient of molecular hydrogen or the appearance of some additional mechanism for mass transport. Judging from the hydrogen concentration at the instant when both curves showing the absorption decay start coinciding, this mechanism becomes significant at loading pressures above 50–60 MPa (500–600 atm). At lower pressures, the hydrogen outlet is described by the standard diffusion equation with a constant coefficient.

3.3 Change in the spectral properties of Bragg gratings

The resonance reflection wavelength λ_{Br} of a FBG written in the fibre core depends on the concentration of molecular hydrogen at the fibre axis [12, 16], but at the same time is not directly related to its vibrational spectrum. The dissolution of molecular hydrogen in the fibre increases the effective refractive index n_{eff} of the fundamental mode and, in accordance with Bragg condition $\lambda_{\text{Br}} = 2n_{\text{eff}}\Lambda$ (where Λ is the grating period), leads to the red shift of the resonance wavelength [12].

Figure 4 shows the transmission spectra of two FBGs written in fibre No. 5 at a distance of 1 cm from each other. According to the writing dynamics, the first grating (Gr1) is type I grating, while the second grating (Gr2) was written before the disappearance of type I grating when type IIa grating had not appeared yet [15]. Figure 4 shows the initial transmission spectrum for this chain of gratings, as well as two spectra measured 5 and 25 h after hydrogen loading (for better visualisation, the spectra are displaced relative to each other by 0.25 dB along the vertical axis).

Note that the presence of dissolved molecular hydrogen considerably affects the average refractive index of the

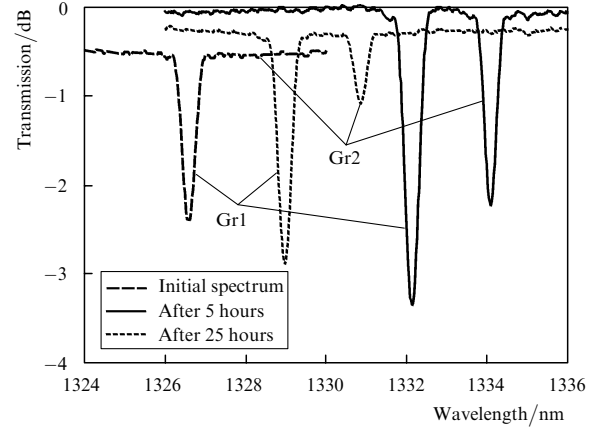


Figure 4. Transmission spectra of FBGs Gr1 and Gr2 written in fibre No. 5, which were measured before hydrogen loading and 5 and 25 hours after its completion. For better visualisation, the spectra are displaced by 0.25 dB relative to one another along the vertical.

grating (resonance wavelength shift) and also leads to a reversible variation in the refractive index modulation amplitude. To our knowledge, this effect was observed for the first time. Note that after the outlet of hydrogen from the fibre, the spectrum is almost completely restored to its initial state (before hydrogen loading) within the measurement error. Hydrogen loading of both types of gratings leads to a change in the modulation amplitude of the refractive index. In the Gr1 grating, the initial modulation amplitude of the refractive index was $\sim 3 \times 10^{-4}$, increasing by $\delta n_{\text{mod}}^{\text{Gr1}} \approx 1 \times 10^{-4}$ after hydrogen loading. In the Gr2 grating, the modulation amplitude in the first diffraction order varied even more significantly, from nearly zero to $\delta n_{\text{mod}}^{\text{Gr2}} \approx 3 \times 10^{-4}$. Note that the difference between the resonance wavelengths of both gratings after hydrogen loading increased by 0.1 nm. This corresponds to the fact that the average value of the refractive index induced in the Gr2 grating was higher than that in Gr1 by $\delta n_{\text{avr}}^{\text{Gr2}} - \delta n_{\text{avr}}^{\text{Gr1}} \approx 1 \times 10^{-4}$, which is nearly the same as $(\delta n_{\text{mod}}^{\text{Gr2}} - \delta n_{\text{mod}}^{\text{Gr1}})/2 \approx 1 \times 10^{-4}$.

The above estimates led to the assumption that an increase in the modulation amplitude of refractive index gratings is due to a higher solubility of hydrogen in the irradiated regions of the fibre than in the unexposed regions. Considering the total shift in the gratings corresponding to a refractive index variation of about 6×10^{-3} , it can be stated that the solubility of hydrogen in the irradiated core regions in a GS fibre with a GeO_2 molar concentration of 24% (sample No. 5) increases after a radiation dose $D = 70 \text{ kJ cm}^{-2}$ at $\lambda = 244 \text{ nm}$ (under Gr2 recording conditions) by about 5% over the value for unexposed regions.

The following mechanism can be proposed for the increase in the solubility of hydrogen in the glass exposed to ultraviolet radiation. Irradiation of GS glass leads to a rearrangement of its network, accompanied by a rupture of bonds and formation of rings with a smaller number of links [17]. Apparently, such a rearrangement takes place as a result of stretching or rupture of weak bonds at the boundaries of clusters forming the glass network. In our opinion, this may lead to a decrease in the average size of clusters accompanied by a simultaneous increase in their density and in the size of regions of lower density between clusters. The latter circumstance may be mainly responsible

for the increase in the solubility of hydrogen in germanosilicate glass subjected to UV irradiation. Further investigations are required for confirming this hypothesis and a better understanding of the observed phenomenon.

Note that the increase in the solubility of hydrogen in the irradiated fibre regions may be manifested even in the case of hydrogen loading at normal pressures (10–15 MPa). In this case, the modulation amplitude of the induced refractive index of the gratings must vary by about 10^{-5} . This circumstance may explain the emergence of the thermally unstable component of the refractive index induced in gratings recorded in the hydrogen-loaded fibres. For example, it was mentioned in [18] that a decrease of about 10% in the induced refractive index occurs at room temperature during the first two weeks after its recording (this approximately corresponds to the time of outlet of molecular hydrogen from the fibre), after which it remained unchanged over a period of six months.

Figure 5 shows the variation of the resonance wavelength of the grating during the outlet of hydrogen from the fibre, measured in fibre No. 4. A good linear dependence observed in this case indicates that even for high concentrations of hydrogen, the variation in the refractive index of silica glass is additive and is not saturated. This circumstance points towards the absence of a strong interaction between the dissolved hydrogen molecules up to molar concentrations of H_2 ($C_{H_2} \sim 10\%$) measured in our experiments. Variation in the average refractive index induced by hydrogen loading for such concentrations at the initial instant of time was about 4.5×10^{-3} , while the shift in the resonance wavelength of the grating was about of 4 nm. The slope of the dependence $\Delta n(C_{H_2})$ was $4.42 \times 10^{-4} (\%)^{-1}$, which is about 1.5 times the value obtained in [9] for planar waveguides.

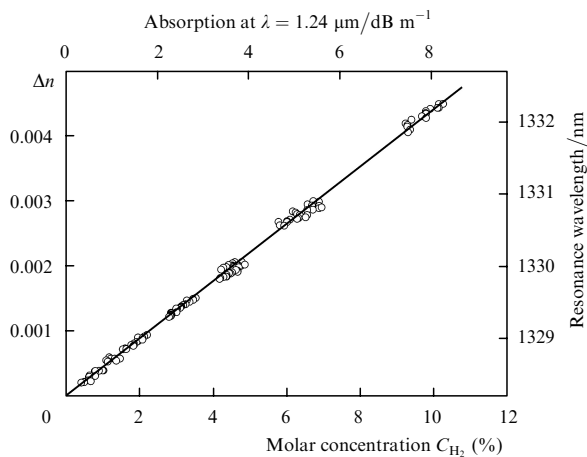


Figure 5. Dependence of the hydrogen-induced refractive index and resonance wavelength of the FBG on the molar concentration C_{H_2} of hydrogen in the glass network of fibre No. 4.

An analogous, but slightly larger (5.5 nm), shift of the grating reflection peak was observed for fibre No. 5 (see Fig. 4). This indicates that the solubility of hydrogen depends on the glass composition (on the concentration of germanium in the core) and increases with it in the case considered here (the solubility in fibre No. 5 is about twice as high). Note that such experimental dependences were also obtained for the measurements of the dynamics of hydrogen

outlet from fibre Nos 2 and 3 in which FBGs were written by pulsed radiation of a KrF excimer laser through a phase mask.

Despite the fact that the above circumstances prevented measurements of changes occurring in individual Raman rotational bands due to outlet of hydrogen, we were able to measure the integrated intensity of the Q_1 band. Its dependence on hydrogen concentration along the fibre axis is shown in Fig. 6. One can see that like the dependence $\Delta n(C_{H_2})$, this dependence is also linear.

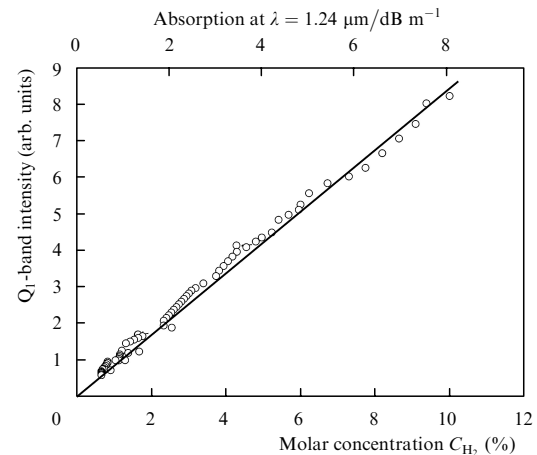


Figure 6. Dependence of integrated intensity of the Q_1 Raman band on the hydrogen concentration in the fibre.

4. Discussion of experimental results

It was shown in the preceding sections that the experimental dependences (amplitude of absorption band at $1.24 \mu\text{m}$, change in the refractive index of glass, and intensity of the Q_1 band in the Raman spectrum) measured during outlet of hydrogen from fibres subjected to high-pressure hydrogen loading are proportional to one another and indicate that the rate of hydrogen outlet from the fibre after hydrogen loading is much higher than at low loading pressures. Only when the concentration of hydrogen in the core falls to the loading level at a pressure of 50 MPa, its further variation corresponds to diffusion with a known constant coefficient and can be described quite well by solving the time-dependent diffusion equation. However, this approach cannot explain the rapid initial outlet of hydrogen observed in our experiments at high loading pressures. Note that we observed rapid outlet of hydrogen in all GS fibres investigated irrespective of the concentration of germanium in the core.

It was mentioned above that rapid outlet of H_2 can be explained by an increase in the diffusion constant upon an increase in the hydrogen concentration in the glass network or by the presence of an additional mechanism of mass transport leading to a faster decrease in hydrogen concentration in the core region at the initial stage.

We believe that the rapid outlet of hydrogen immediately after completion of hydrogen loading is due to the contribution from barodiffusion [19, 20] associated with radial gradients of the hydrogen pressure P_{H_2} in the fibre. In the presence of a pressure gradient, the flux density J of diffusing particles is expressed by the relation

$$J = -D_{\text{H}_2} [\text{grad } C_{\text{H}_2} + \alpha_P \text{grad}(\ln P_{\text{H}_2})], \quad (1)$$

where D_{H_2} is the diffusion coefficient for hydrogen molecules and α_P is the barodiffusion ratio.

At a low concentration of hydrogen molecules, they collide mainly with the atoms of the glass network during their motion. Hence hydrogen pressure gradients do not affect the overall mass transport (the first term in Eqn (1) predominates). Such a situation is realised when the average number of H_2 molecules in the interstices of the glass network is much smaller than unity. Hence we can consider an equation containing only the first term while studying the hydrogen diffusion processes in fibres at low pressures. It was shown above that upon an increase in the loading pressure to 100–200 MPa, the concentration of hydrogen dissolved in the fibre is no longer strictly proportional to this pressure, thus pointing towards the appearance of mutual interaction between molecules due to an increase in their concentration in the glass network. This means that the average number of H_2 molecules in the interstices of the network becomes comparable with unity but, according to our estimates, does not exceed it. For such a high concentration of H_2 molecules ($\sim 3 \times 10^{21} \text{ cm}^{-3}$), the frequency of collisions between molecules becomes comparable with the frequency of their collisions with atoms of the network and the presence of a pressure gradient in any preferred direction results in the emergence of a flow of H_2 molecules in a direction opposite to this gradient. The flux described by the second term in Eqn (1) in the case considered by us becomes comparable with the normal diffusion flux of hydrogen molecules.

Figure 7 shows the experimental dynamics of hydrogen concentration in the core of fibre No. 4, measured from the dependence of the amplitude of the 1.24- μm absorption band. This dependence was used to optimise the dimensionless coefficient α_P under the assumption that it is proportional to a power function of hydrogen concentration, i.e., has the form $\alpha_P = A\bar{C}_{\text{H}_2}^B$. Calculations were made by using the relative hydrogen concentration $\bar{C}_{\text{H}_2} = C_{\text{H}_2}(t)/C_{\text{H}_2}(0)$. The best agreement between the theoretical and experimental curves describing the hydrogen outlet was attained for $A = 3.5 \pm 0.5$ and $B = 4 \pm 0.5$. The corresponding dependence is shown by the solid curve in Fig. 7. Note that the power function of concentration used for calculating α_P leads to a very good approximation of the observed

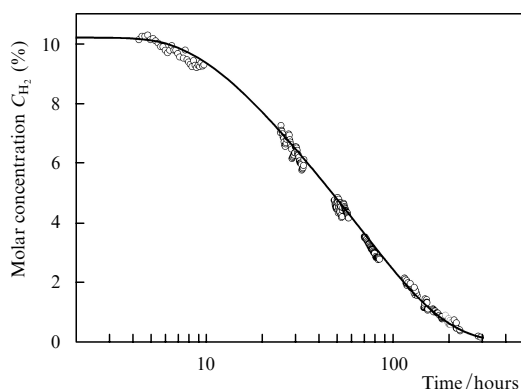


Figure 7. Decay of the molecular hydrogen concentration along the fibre axis measured experimentally (circles) and calculated by taking barodiffusion into account (solid curve).

experimental dependences. It should also be remarked that the barodiffusion coefficient increases rapidly with hydrogen concentration in the glass network.

5. Conclusions

We have studied the Raman and absorption bands for H_2 molecules in single-mode GS glass fibres loaded with hydrogen at pressures of 150–170 MPa. Loading of fibres to such pressures made it possible to observe for the first time purely rotational S_0 -branch transitions in the Raman spectra of molecular hydrogen dissolved in silica glass. It was found that an increase in the concentration of H_2 in glass leads to the blue shifts of the vibrational Q_1 band in the Raman spectrum and the 1.24- μm absorption band.

A rapid initial stage was observed for the first time in the dynamics of variation of spectral parameters of the absorption and Raman bands of H_2 molecules as well as the characteristics of FBGs during the outlet of hydrogen from the fibre. This effect was observed for all investigated optical fibres and was independent of the germanium concentration in the core. It is shown that this effect can be due to the contribution of barodiffusion of H_2 molecules, associated with the radial pressure gradient of hydrogen at its high concentrations in the glass network.

In our opinion, we observed for the first time the effect of molecular hydrogen dissolved in the glass network not only on the spectral position of the resonance wavelength of FBGs, but also on the modulation amplitude of the refractive index. Apparently, the latter effect is due to a higher solubility in the fibre regions exposed to UV radiation.

Note that the effects and regularities observed in the course of our investigations, which are associated with the high concentration of hydrogen loaded into the fibres, should be taken into account while analysing optical losses in the telecommunication spectral range, and also while recording photoinduced refractive index gratings in them, on account of a high photosensitivity of fibres subjected to such a treatment.

Acknowledgements. The authors thank A.S. Biryukov for useful discussions of the results obtained in this study. This research was supported by the Russian Foundation for Basic Research (Grant Nos 01-01-16848, 04-02-17025 and 03-02-16201) and by the Moscow Committee on Science and Technology (Grant No. 1.2.30, 2004).

References

1. Lemaire P.J. *Opt. Eng.*, **30**, 780 (1991).
2. Stone J. J. *Lightwave Technol.*, **5**, 712 (1987).
3. Lemaire P.J., Atkins R.M., Mizrahi V., Reed W.A. *Electron. Lett.*, **29**, 1191 (1993).
4. Starodubov D.S., Dianov E.M., Vasiliev S.A., Frolov A.A., Medvedkov O.I., Rybaltovskii A.O., Titova V.A. *Proc. SPIE Int. Soc. Opt. Eng.*, **2998**, 111 (1997).
5. Brennan J.F., Sloan D., Dent J., LaBrake D. *Proc. Conf. Opt. Fib. Commun.*, **3**, 59 (1999).
6. Grubsky V., Starodubov D.S., Feinberg J. *Opt. Lett.*, **24**, 729 (1999).
7. Cordier P., Dalle C., Depecker C., Bernage P., Douay M., Niay P., Bayon J.-F., Dong L. *J. Non-Cryst. Sol.*, **224**, 277 (1998).

8. Plotnichenko V.G., Rybaltovskii A.O., Sokolov V.O., Koltashev V.V., Malosiev A.R., Popov V.K., Dianov E.M. *J. Non-Crys. Sol.*, **281**, 25 (2001).
9. Faerch K., Svalgaard M. *Proc. Conf. BGPP'2003* (Monterey, USA, 2003) Vol.178, paper TuA2.
10. Hartwig C.M. *J. Appl. Phys.*, **47**, 956 (1976).
11. Schmidt B.C., Holtz F.M., Beny J.-M. *J. Non-Crys. Sol.*, **240**, 91 (1998).
12. Malo B., Albert J., Hill K.O., Bilodeau F., Johnson D.C. *Electron. Lett.*, **30**, 442 (1994).
13. Hill K.O., Malo B., Bilodeau F., Johnson D.C., Albert J. *Appl. Phys. Lett.*, **62**, 1035 (1993).
14. Medvedkov O.I., Korolev I.G., Vasil'ev S.A. Preprint (6) (Moscow, A.M. Prokhorov General Physics Institute, 2004).
15. Xie W.X., Niay P., Bernage P., Douay M., Bayon J.F., Georges T., Monerie M., Poumellec B. *Opt. Commun.*, **104**, 185 (1993).
16. Fu L.B., Tan G., Xu W.J., An H.L., Cui X.M., Lin X.Z., Liu H.D. *Opt. Lett.*, **25**, 527 (2000).
17. Dianov E.M., Plotnichenko V.G., Koltashev V.V., Pyrkov Yu.N., Ky N.H., Limberger H.G., Salathe R.P. *Opt. Lett.*, **22**, 1754 (1997).
18. Patrick H., Gilbert S.L., Lidgard A., Gallagher M.D. *J. Appl. Phys.*, **78**, 2940 (1995).
19. Hirschfelder J., Curtiss Ch., Bird R. *Molecular Theory of Gases and Fluids* (New York: John Wiley and Sons, 1954; Moscow: Inostrannaya Literatura, 1961).
20. Landau L.D., Lifshitz E.M. *Fluid Mechanics* (New York, Oxford: Pergamon Press, 1987; Moscow: Nauka, 1988).